

Universal nucleation length for slip-weakening rupture instability under nonuniform fault loading

Koji Uenishi and James R. Rice

Department of Earth and Planetary Sciences and Division of Engineering and Applied Sciences, Harvard University, Cambridge, Massachusetts, USA

Received 28 November 2001; revised 8 June 2002; accepted 8 October 2002; published 25 January 2003.

[1] We consider the nucleation of instability on a slip-weakening fault subjected to a heterogeneous, locally peaked “loading” stress. That stress is assumed not only to gradually increase due to tectonic loading but also to retain its peaked character. The case of a linear stress versus slip law is considered in the framework of two-dimensional quasi-static elasticity for a planar fault. Slip initiates when the peak of the loading stress first reaches the strength level of the fault to start slip weakening. Then the size of the slipping region grows under increased loading stress until finally a critical nucleation length is reached, at which no further quasi-static solution exists for additional increase of the loading. That marks the onset of a dynamically controlled instability. We prove that the nucleation length is independent of the shape of the loading stress distribution. Its universal value is proportional to an elastic modulus and inversely proportional to the slip-weakening rate, and it is given by the solution to an eigenvalue problem. That is the same eigenvalue problem introduced by Campillo, Ionescu, and collaborators for dynamic slip nucleation under spatially uniform prestress on a fault segment of fixed length; the critical length that we derive is the same as in their case. To illustrate the nucleation process, and its universal feature, in specific examples, we consider cases for which the loading stress is peaked symmetrically or nonsymmetrically, and we employ a numerical approach based on a Chebyshev polynomial representation. Laboratory-derived and earthquake-inferred data are used to evaluate the nucleation size. *INDEX TERMS*: 3210 Mathematical Geophysics: Modeling; 7209 Seismology: Earthquake dynamics and mechanics; 7215 Seismology: Earthquake parameters; 7230 Seismology: Seismicity and seismotectonics; 7260 Seismology: Theory and modeling; *KEYWORDS*: earthquake nucleation, slip weakening, fault instability

Citation: Uenishi, K., and J. R. Rice, Universal nucleation length for slip-weakening rupture instability under nonuniform fault loading, *J. Geophys. Res.*, 108(B1), 2042, doi:10.1029/2001JB001681, 2003.

1. Introduction

[2] Understanding the earthquake nucleation process is of fundamental importance for earthquake physics and has practical implications. The purpose of this study is to identify the factors that control the nucleation of two-dimensional in-plane or antiplane slip-weakening instabilities, and to evaluate the nucleation length that is relevant to fault instabilities and earthquake rupture. We consider a planar fault that is under a locally peaked heterogeneous “loading” stress. This loading stress is assumed to gradually increase due to tectonic loading but to retain its peaked character. The case of a linear slip-weakening constitutive law is considered in the framework of two-dimensional quasi-static elasticity. The size of the slipping region on the fault grows under increased loading stress until finally a critical nucleation length is reached at which no further quasi-static solution exists. That marks the onset of a dynamically controlled instability.

[3] Analytically as well as numerically, models based on slip-weakening or rate- and state-dependent constitutive laws have been developed and used to investigate the initiation process of earthquakes and especially the transition from stable quasi-static growth of the size of the slip-rupturing zone to unstable high speed rupture propagation [e.g., *Tse and Rice*, 1986; *Okubo*, 1989; *Dieterich*, 1992; *Rice and Ben-Zion*, 1996; *Shibasaki and Matsu'ura*, 1998; *Ohnaka*, 2000]. Numerically, this type of problem has had difficulties, because the conventional quasi-static methods, used for simulating slow deformational processes of long duration, fail as instabilities develop. Recently, however, *Lapusta et al.* [2000] developed an efficient numerical procedure, in the context of rate and state friction, for calculating the elastodynamic response of a fault subjected to slow tectonic loading processes of long duration within which there are episodes of rapid earthquake failure; that has recently been applied (*N. Lapusta and J. R. Rice*, Nucleation and early seismic propagation of small and large events in a crustal earthquake model, submitted to *Journal of Geophysical Research*, 2002, hereinafter referred to as *Lapusta and Rice*, submitted manuscript, 2002) to study of

nucleation under the spatially nonuniform stresses which develop in simulations of sequences of events.

[4] Analytically, based on the potential energy principle in quasi-static elasticity and the assumption of a linear displacement-softening law (analogous to slip-weakening for shear rupture), *Li and Liang* [1993] have introduced a boundary eigenvalue problem for a cohesive crack model. They have indicated that under a critical condition associated with the smallest eigenvalue, the corresponding eigenfunction represents the nonunique part of the displacement solution and the critical load can be determined via the eigenfunction. By variational analysis, *Bazant and Li* [1995a, 1995b] have obtained the condition of stability loss of an elastic structure with a growing cohesive crack in which the cohesive stress is a specified decreasing function of the crack opening displacement, and transformed it into an eigenvalue problem for a homogeneous Fredholm integral equation, with the structure size as the eigenvalue. Under the assumption of a linear displacement-softening relation for the cohesive crack, they have solved for the maximum load as well as the maximum deflection that is carried by the structure, explicitly in terms of the eigenfunction associated with the integral equation.

[5] By means of a spectral analysis, *Campillo and Ionescu* [1997] have investigated the initiation of dynamic antiplane slip instabilities of a slip-weakening fault in a homogeneous linear elastic medium that is prestressed uniformly up to the frictional threshold. In the analysis, an analytical expression of the slip, which can be interpreted using an eigenvalue analysis, has been given and divided into two parts: the solution associated with positive eigenvalues (“dominant part”) and negative eigenvalues (“wave part”). It has been shown that the dominant part, characterized by an exponential growth with time, controls the development of the instability and the wave part becomes rapidly negligible when the instability develops. The effect of slip-weakening rate on the duration of the nucleation phase and the critical fault length has been evaluated [*Campillo and Ionescu*, 1997; *Ionescu and Campillo*, 1999]. The analysis has been further extended to in-plane shear instabilities [*Favreau et al.*, 1999] and to instabilities of a finite fault of (a priori) fixed length [*Dascalu et al.*, 2000]. However, no explanation regarding the physical meaning of the (a priori) fixed fault length and uniform loading has been given in these analyses, and rigorous numerical treatments of the complete earthquake cycle [*Lapusta et al.*, 2000; *Lapusta and Rice*, submitted manuscript, 2002] show clearly that a region of initially aseismic slip grows in size in a quasi-static manner before dynamic breakout of the rupture.

[6] In the following, based on the quasi-static elastic equilibrium condition and the linear slip-weakening friction law, we show that the problem of slip-weakening instabilities can be reduced to an eigenvalue problem. The analysis indicates that the nucleation length relevant to the instabilities is universal. It depends only on elastic modulus of the medium and the slip-weakening rate, and it is not influenced by the (slow) rate of increase of loading stress, or by the functional form of dependence of the decrease of loading stress, away from its peak value, on position along the fault. The critical increment of the peak loading stress, above the peak stress at which slip-weakening initiates, is given in a simple, mathematical expression in terms of the associated

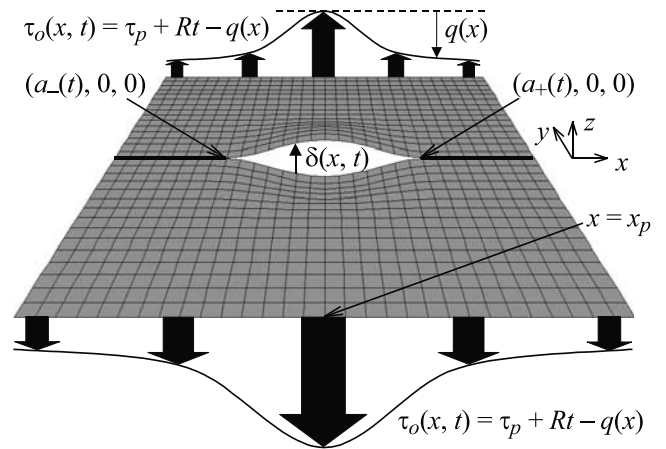


Figure 1. A displacement field associated with antiplane shear (mode III) rupture in an infinite, homogeneous, linear elastic space. The loading shear stress $\tau_o(x, t)$ is locally peaked in space and increases gradually with time, at rate R . Similarly, we can define the problem for in-plane shear (mode II), or for tensile (mode I) rupture.

eigenvalues and eigenfunctions. Then, by means of a Chebyshev polynomial representation, we numerically investigate the slip development on the slip-weakening fault for some specific loading distributions, and confirm the analytical results. Although the problem considered here is quite simplified, it still retains the fundamental features that are believed to play a crucial role during the nucleation process. This universal length of the slip-weakening zone size at instability is valid only for linear slip weakening, that is, is valid so long as the maximum slip on the fault at instability is small enough to allow use of a law with linear decrease of strength with slip. Further, we emphasize that slip-weakening must be regarded as an approximation to more precise descriptions of friction in the rate and state framework. We adopt a slip-weakening model here, particularly in linear form, because it has been used widely in earlier studies and because we have been able to derive the remarkable result of a universal nucleation length for that case, under arbitrarily variable prestress, which suggests new connections with, and interpretations of, some of that earlier work.

2. Problem Statement

[7] We consider fault rupture in an infinite, homogeneous elastic space subjected to a locally peaked loading stress, $\tau_o = \tau_o(x, t)$. The fault plane coincides with the x - z plane ($y = 0$) of a Cartesian coordinate system xyz . The only nonzero displacement is $u_z(x, y, t)$ for antiplane (mode III) shearing, or $u_x(x, y, t)$ for in-plane (mode II) shearing, or $u_y(x, y, t)$ for tensile (mode I) loading, where t is time ($t \geq 0$). We define slip $\delta(x, t)$ on the fault plane as the displacement discontinuity $\delta(x, t) = u_z(x, 0^+, t) - u_z(x, 0^-, t)$ for mode III, or $u_x(x, 0^+, t) - u_x(x, 0^-, t)$ for mode II, and understand δ as the tensile opening $u_y(x, 0^+, t) - u_y(x, 0^-, t)$ for mode I. The relevant shear (or tensile) stress on the fault plane is denoted by $\tau(x, t)$ and coincides with $\sigma_{yz}(x, 0, t)$ for mode III, $\sigma_{xy}(x, 0, t)$ for mode II, and $\sigma_y(x, 0, t)$ for mode I. Figure 1 shows the situation for a shearing mode.

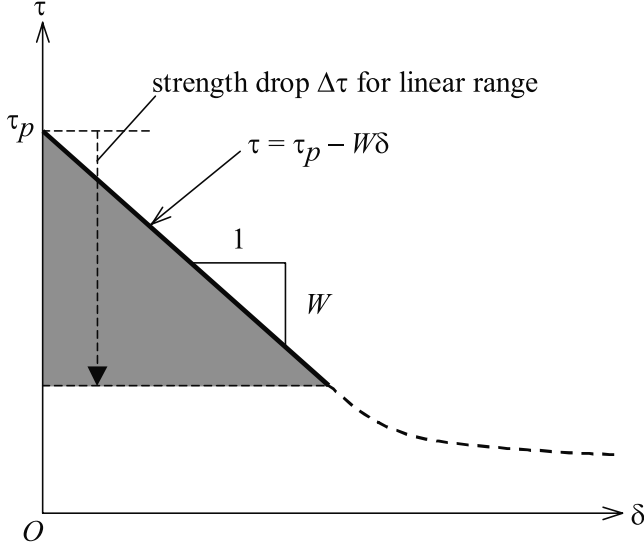


Figure 2. The (initially) linear slip-weakening constitutive law. The stress inside the slipping region of the fault obeys the linear relation $\tau = \tau_p - W\delta$, at least when the strength drop is less than $\Delta\tau$. The slip-weakening rate W is a constant ($W > 0$).

[8] By considering the quasi-static elastic equilibrium, we can express the stress on the fault plane $\tau(x, t)$ only in terms of the slip $\delta(x, t)$ as [e.g., *Bilby and Eshelby, 1968*]

$$\tau(x, t) = \tau_o(x, t) - \frac{\mu^*}{2\pi} \int_{a_-(t)}^{a_+(t)} \frac{\partial\delta(\xi, t)/\partial\xi}{x - \xi} d\xi, \quad (1)$$

where $\mu^* = \mu$ (shear modulus) for mode III and $\mu/(1 - \nu)$ for modes I and II, with ν being Poisson's ratio. The slipping region $a_-(t) < x < a_+(t)$ is slowly expanding, and the quasi-statically increasing loading stress $\tau_o(x, t)$, which is locally peaked at $x = x_p$, is the stress that would act if the fault was constrained against any slip (or opening). It is assumed that $\tau_o(x, t)$ takes the form

$$\tau_o(x, t) = \tau_p + Rt - q(x). \quad (2)$$

Here, τ_p is the shear (for modes II and III) or tensile (for mode I) strength of the fault, and $R (> 0)$ is the loading rate of the increasing stress. The function $q(x)$ satisfies $q(x) > 0$ for $x \neq x_p$ and $q(x_p) = 0$. Thus $t = 0$ is the time when the peak value of loading stress, at x_p , first reaches τ_p so that slip initiates at that point. Figure 1 shows a typical symmetric distribution of the loading stress $\tau_o(x, t)$ for the antiplane shearing case.

[9] In most of this study, as a constitutive law inside the slipping region, we employ the slip-weakening friction law

$$\tau(x, t) = \tau_p - W\delta(x, t), \quad (3)$$

where τ_p is the peak strength (i.e., the friction threshold for the shear modes), and we consider sufficiently small slip δ so that a linear slip-weakening law with constant weakening rate W ($W > 0$) applies at least approximately for the range of slips which occur prior to instability. Figure 2 shows schematically this friction law (3). In the figure, the ordinate denotes the stress τ and the abscissa corresponds to the slip δ . Slip can occur if the local shear stress reaches the peak

shear strength τ_p . (In a mode I interpretation, fracture opening can occur if tensile stress reaches τ_p .) The stress inside the slipping region of the fault drops according to the linear relation (3). From the elastic equilibrium condition (1) and the slip-weakening friction law (3), together with equation (2), we obtain

$$-W\delta(x, t) = Rt - q(x) - \frac{\mu^*}{2\pi} \int_{a_-(t)}^{a_+(t)} \frac{\partial\delta(\xi, t)/\partial\xi}{x - \xi} d\xi, \quad (4)$$

when $\delta > 0$, that is, for $a_-(t) < x < a_+(t)$.

[10] Figure 3 shows schematically the development of the slipping region by the increasing loading stress. (The first diagram) pertains to the situation at time $t = 0$, where the loading stress $\tau_o(x, 0)$ reaches the strength of the fault, τ_p , to start slip weakening. Prior to this stage, no slip has occurred. The function $q(x)$ can be identified as the difference between the straight horizontal line $\tau = \tau_p$ and the curve $\tau = \tau_o(x, 0)$. At $t > 0$ (middle diagram), part of the fault slips and the stress inside the slipping region drops according to the slip-weakening friction law (3). Note that the extremities of the quasi-static slipping region where $\delta > 0$ (i.e., the support of the slip distribution) are not specified a priori and will automatically be chosen so that the quasi-statically calculated $\tau(x, t) = \tau_p$ is satisfied at those extremities, $x = a_{\pm}(t)$. At least that will hold so long as a quasi-static solution actually exists. We would like to know when it just fails to exist; this situation gives the nucleation length of earthquake rupture. The last diagram shows such a situation. At a late stage, a critical nucleation length h_n is reached at which no further quasi-static solution exists for additional increase of the loading. That marks the onset of a dynamically controlled instability. In the following, we will prove that for the linear displacement-weakening law, the nucleation length is independent of the shape of the loading stress distribution, that is, it is independent of the mathematical form of $q(x)$. Its universal value is proportional to an elastic modulus and inversely proportional to the displacement-weakening rate, and is given by the solution to an eigenvalue problem. To illustrate the nucleation process, and its universal feature, in specific examples, we consider cases for which the loading stress is peaked symmetrically or nonsymmetrically, and employ a numerical approach based on a Chebyshev polynomial representation. Laboratory-derived and earthquake-inferred data are used to evaluate the nucleation size.

3. Universal Nucleation Length Under Locally Peaked Loading

3.1. Dimensional Analysis; Comparison of Linear and Nonlinear Slip-Weakening Laws

[11] First, we give a dimensional analysis of the problem which already hints at a universal nucleation length in the linearly weakening case like in Figure 2, by showing that for a specific one-parameter form of $q(x)$, the nucleation length is independent of that parameter. This analysis also shows that a universal nucleation length is not to be expected when weakening on the fault cannot be described by a linear law.

[12] We perform dimensional analysis of the nucleation problem for the quadratic form of the loading function, $q(x) = \kappa x^2/2$. Here κ is a positive constant corresponding to the curvature of $q(x)$, with the dimension of Pa/m^2 . Letting $\mu^*\delta$ be the slip-like variable in equation (4), the independent

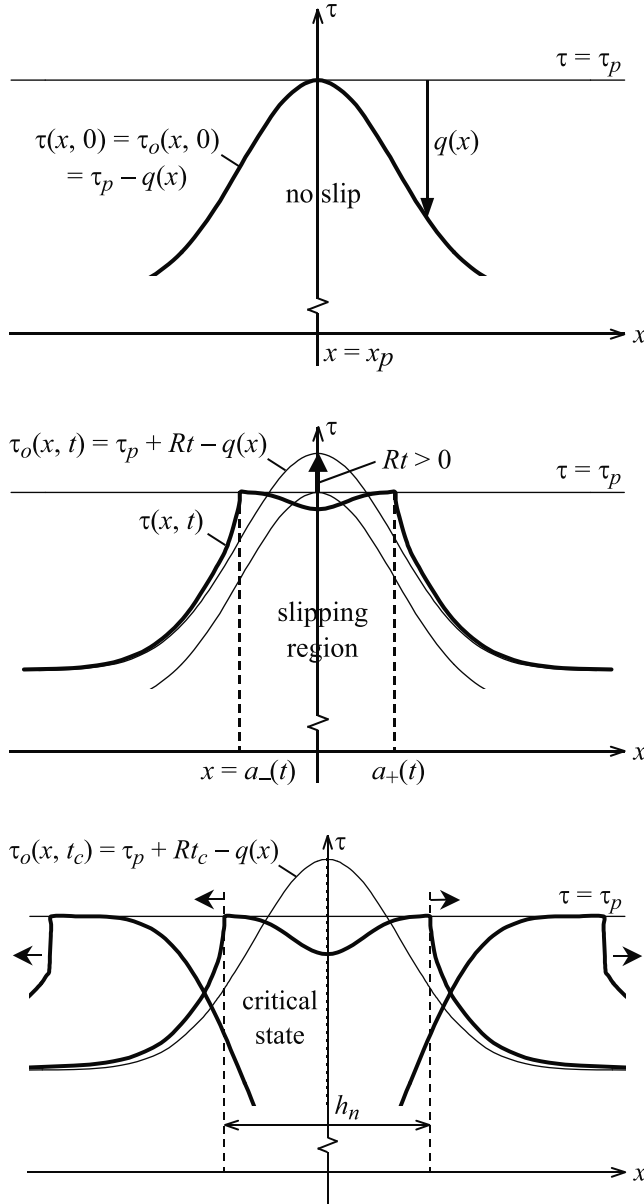


Figure 3. Development of the slipping region induced by the increasing loading stress. (top) At time $t = 0$, the peak of the stress distribution reaches the peak strength of the fault, τ_p . Prior to this stage, no slip has occurred; (middle) At $t > 0$, part of the fault slips and the stress inside the slipping region drops according to the slip-weakening friction law; and (bottom) At a later stage, when the length of the slipping region reaches a critical value, h_n , the fault system becomes unstable and the slipping region will expand even without any increase of the loading stress. We will show that h_n is independent of R and $q(x)$.

parameters of the problem are the ratio of slip-weakening rate to the shear modulus W/μ^* [1/m] and the curvature κ [Pa/m²]. Each stage of the dimensional analysis is listed in Table 1.

[13] Originally we have two dependent variables, the nucleation length h_n [m] and the critical stress increment Rt_c [Pa], and two independent ones, W/μ^* [1/m] and κ [Pa/m²] (see the first row of Table 1). When we remove the dimension

of length [m] from the variables, we have new variables $h_n W/\mu^*$ [dimensionless] and $\kappa \mu^{*2}/W^2$ [Pa] (second row). We further eliminate the dimension of stress [Pa] and finally have two dimensionless dependent variables, $h_n W/\mu^*$ and $Rt_c W^2/(\kappa \mu^{*2})$ (bottom row), and no remaining independent variables. This result shows that

$$h_n W/\mu^* = \text{constant, and } Rt_c W^2/(\kappa \mu^{*2}) = \text{constant.} \quad (5)$$

Equation (5) shows that $h_n W/\mu^*$ is universal, i.e., independent of the curvature, κ , and also $Rt_c/(\kappa h_n^2)$ is a constant. Note that if we added additional parameters, necessarily of length dimensions, in the definition of $q(x)$, then it would not be obvious from dimensional analysis that h_n is universal, a result proven below.

[14] In the case of the nonlinear power-type slip-weakening law

$$\tau = \tau_p - A\delta^n, \quad (6)$$

with A and n being positive constants, dimensional analysis suggests that there is no universal nucleation length when $n \neq 1$, even for the case $q(x) = \kappa x^2/2$. In that case, if there exists a nucleation length h_n , both h_n and the critical stress increment Rt_c depend on the curvature κ and they are given by

$$h_n = f(n) \frac{\kappa^{(1-n)/(3n-2)} \mu^{*n/(3n-2)}}{A^{1/(3n-2)}} \text{ and } Rt_c = g(n) \kappa h_n^2, \quad (7)$$

where $f(n)$ and $g(n)$ are presently undetermined functions of n .

[15] Our preliminary analytical calculations using an energy approach [Rice and Uenishi, 2002] show that for $n < 2/3$, the system described by this mathematical representation is unstable as soon as the loading stress reaches τ_p at a single point ($dt/da < 0$ near $a = 0^+$). However, as we discuss below, the seismic [Abercrombie and Rice, 2001] and laboratory [Chambon et al., 2002] evidence suggesting a slip-weakening law approximately in that form, with n in the range $n < 2/3$, is for slips that are already much larger than those inferred, from laboratory studies, to lead to nucleation. So there is no inconsistency, in that the highly unstable power law describes response after nucleation. This is somewhat like the assumption of two weakening scales [Shaw and Rice, 2000], i.e., a large slip-weakening rate W for small slip δ at which nucleation occurs, and further weakening, possibly due to a thermal effect, with smaller W for much larger δ developing during unstable slip.

3.2. Universal Nucleation Length

[16] Returning to the linear case, at each loading stress increment, the extremities of the quasi-static slipping region get chosen precisely to remove the singularity at the

Table 1. Independent and Dependent Variables and Their Dimensions

Dependent		Independent	
h_n [m]	Rt_c [Pa]	W/μ^* [1/m]	κ [Pa/m ²]
$h_n W/\mu^*$ [0]	Rt_c [Pa]	$\kappa \mu^{*2}/W^2$ [Pa]	
$h_n W/\mu^*$ [0]	$Rt_c W^2/(\kappa \mu^{*2})$ [0]		

ends [$x = a_{\pm}(t)$]. The condition that we have no singularity of stress at these ends implies (see Appendix A for details)

$$\partial\delta(x, t)/\partial x \sim \sqrt{\pm[a_{\pm}(t) - x]} \quad \text{for } x \text{ near } a_{\pm}(t), \quad (8)$$

where here the \sim symbol means “is of the order of” as the right side approaches zero. This relation justifies that, in taking the time derivative of equation (4), the differentiation can be taken inside the integral and operate on the term $\partial\delta(\xi, t)/\partial\xi$. Thus we differentiate equation (4) with respect to time and obtain

$$\begin{aligned} -W V(x, t) &= R - \frac{\mu^*}{2\pi} \int_{a_-(t)}^{a_+(t)} \frac{\partial V(\xi, t)/\partial\xi}{x - \xi} d\xi \\ &\text{for } a_-(t) < x < a_+(t). \end{aligned} \quad (9)$$

Here, $V(x, t)$ is slip rate $V(x, t) \equiv \partial\delta(x, t)/\partial t$. From equation (8), for x near $a_{\pm}(t)$, $V(x, t) \sim \sqrt{\pm[a_{\pm}(t) - x]} da_{\pm}(t)/dt$. Therefore $V(x, t)$ is bounded at the ends of the slipping region if $da_{\pm}(t)/dt$ is bounded, but $V(x, t)$ of the quasi-static analysis becomes unbounded at the nucleation point when at least one of $da_{\pm}(t)/dt$ approaches infinity.

[17] By introducing $a(t) \equiv [a_+(t) - a_-(t)]/2$, $b(t) \equiv [a_+(t) + a_-(t)]/2$, $X \equiv [x - b(t)]/a(t)$ and $v(X, t) \equiv V(x, t)/[\sqrt{2}V_{rms}(t)]$, where $V_{rms}(t)$ is the rootmean square slip rate

$$V_{rms}(t) \equiv \sqrt{\frac{1}{a_+(t) - a_-(t)} \int_{a_-(t)}^{a_+(t)} V^2(x, t) dx}, \quad (10)$$

we can normalize equation (9). Thus, suppressing explicit reference to the time-dependence of $a(t)$, $V_{rms}(t)$ and $v(X, t)$,

$$-\frac{aW}{\mu^*} v(X) = \frac{a}{\sqrt{2}\mu^* V_{rms}} R - \frac{1}{2\pi} \int_{-1}^{+1} \frac{v'(s)}{X - s} ds \quad \text{for } -1 < X < +1, \quad (11)$$

where $'$ denotes the first derivative of a function. Note that $v(X)$ always satisfies $\int_{-1}^{+1} v^2(X) dX = 1$. The slipping region keeps growing in time but since $V_{rms}/(aR/\mu^*)$ diverges as the nucleation condition is approached, at the critical length, $aR/(\mu^* V_{rms})$ becomes zero. That length is the nucleation length that we seek. At that length the above integral equation for $v(X)$ becomes

$$\frac{aW}{\mu^*} v(X) = \frac{1}{2\pi} \int_{-1}^{+1} \frac{v'(s)}{X - s} ds \quad \text{for } -1 < X < +1. \quad (12)$$

The critical length is thus given as the length such that the eigen equation (12) has a nontrivial solution for $v(X)$. Equation (12), together with the specific features of the eigenfunctions summarized in Appendices B and D3, indicates that a solution is given when $a(t)W/\mu^*$ reaches the smallest eigenvalue $a_c W/\mu^* = \lambda_0 \approx 0.579$ and $v(X, t_c)$ is equal to the associated eigenfunction $v_0(X)$. Thus, the critical length h_n is given by

$$h_n = 2a_c \approx 1.158 \mu^*/W. \quad (13)$$

Note that, the critical length depends only on the shear modulus μ^* and the slip-weakening rate W and is independent of the rate and the shape of the loading, that

is, of R and $q(x)$. However, the critical tectonic stress increment Rt_c during which there is quasi-static fault slip, and at the end of which the fault becomes unstable, is dependent on the loading distribution. In Appendix C, we show that Rt_c is given by

$$Rt_c = Q_0(a_c, b_c)/\beta_0, \quad (14)$$

where β_0 and $Q_0(a, b)$ are defined by $\beta_0 \equiv \int_{-1}^{+1} v_0(X) dX$ and $Q_0(a, b) \equiv \int_{-1}^{+1} q(aX + b)v_0(X) dX$, respectively. (We show further that $\partial Q_0(a, b)/\partial b = 0$ at $a = a_c, b = b_c$.) Note that in the case of a symmetrically peaked loading, $q(x) = q(-x)$, $b = 0$ and equation (14) gives an explicit solution once the eigenfunction, which is independent of $q(x)$, is known. We evaluate $v_0(X)$ numerically in Appendix D3, showing there that $\beta_0 \approx 1.332$ and expressing $v_0(X)$, adequately for all practical purposes, as the first three terms of an infinite series. Using that result, we find for all symmetrically peaked loadings that

$$Rt_c \approx 1.502 \int_0^1 q(a_c X) (0.925 - 0.308X^2) \sqrt{1 - X^2} dX. \quad (15)$$

Note that the more nonuniform the loading stress is over the characteristic length a_c , i.e., the greater is $q(a_c X)$, the greater is the increment Rt_c of tectonic loading over which quasi-static slip-weakening occurs. Conversely, if $q(a_c X)$ is small for all X on $0 \leq X \leq 1$, so is Rt_c .

[18] The above eigen equation (12) takes the same form as that found by *Dascalu et al.* [2000] for dynamic slip nucleation under spatially uniform prestress on a fault segment of (a priori) fixed length; the critical length we derive, equation (13) is the same as in their case. (A more precise value of the smallest eigenvalue is suggested by them to be $\lambda_0 = 0.57888694$.) In our analysis, however, the extremities of the slipping region are not specified a priori and the slowly increasing loading stress takes an arbitrary form except for the condition that it is locally peaked. It is plausible that our nucleation length, in the case of a very gently peaked loading stress, that is almost uniform, might coincide with their critical length. However, we find a much stronger result; the length always coincides, no matter how peaked is the loading stress or of what functional form, so long as we are in the linear range of the slip-weakening law.

4. Some Examples

[19] Here, slip development and the critical condition will be examined by assuming three specific loading distributions of $q(x)$. The problem is considered in terms of a Chebyshev polynomial representation described in Appendix D. This appendix shows that we can obtain the slip distribution at each time by solving the following simultaneous equations

$$b_m = \sum_{n=1}^{\infty} A_{mn} u_n(t), \quad (16)$$

where $x_o = a(t)\cos\omega$ and $\delta(x_o, t) = \sum_{n=1}^{\infty} u_n(t) \sin(n\omega)$ ($0 < \omega < \pi$) with $x_o \equiv x - b(t)$. The components of the matrix \mathbf{A} and the vector \mathbf{b} are given in Appendix D2.

4.1. Symmetrically Peaked Loading

[20] Suppose that the loading stress is symmetrically peaked at $x = 0$, i.e., $q(x) = q(-x)$, $q(x) > 0$ for $x \neq 0$ and

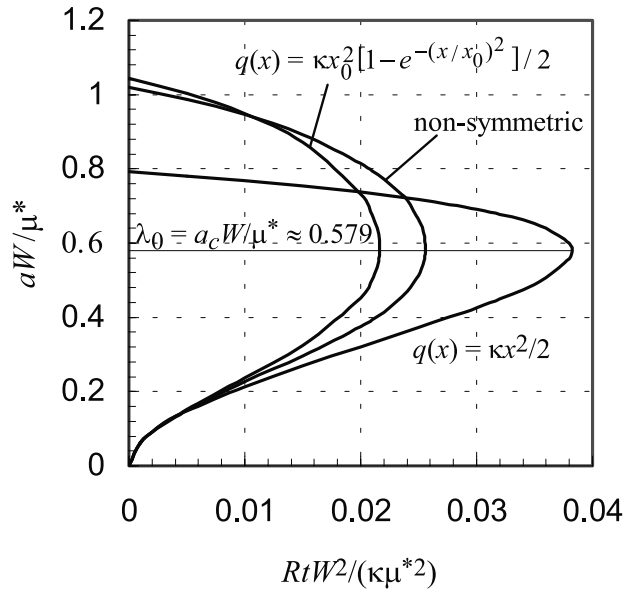


Figure 4. The development of the slipping region half-length a for three different loading distributions of $q(x)$. The parameter $x_0W/\mu^* = 1/3$ for $q(x) = \kappa x_0^2 [1 - e^{-(x/x_0)^2}]/2$ and for the nonsymmetric loading case. Only the lower branches of the curves are physically meaningful if the loading stress is monotonically increasing in time. Instability occurs when the slope becomes unbounded (right extremities of the curves; $da(t)/dt \rightarrow \infty$) all of which correspond to the same nucleation size.

$q(0) = 0$. In this case, the center of the slipping region, $b(t) \equiv [a_+(t) + a_-(t)]/2$, is always located at $b(t) = 0$, with the ends situated at $a_+(t) = -a_-(t) = a(t)$.

[21] First, assume that $q(x)$ is in a quadratic form $q(x) = \kappa x^2/2$. Here $\kappa (>0)$ is a constant that corresponds to the curvature of the function $q(x)$ and has the dimension of Pa/m^2 . Figures 4 and 5 show the development of the half-length of the slipping region, $a(t)W/\mu^*$, and $W^3\delta_{cent}/(\kappa\mu^{*2})$, respectively, where δ_{cent} is the slip at the center of the slipping region ($x = 0$). Note that our analysis is valid only when the slip-weakening law can be modeled as linear for slips that are at least as large as δ_{cent} , evaluated at t_c . The abscissa in the figures denotes the normalized stress increment, $RtW^2/(\kappa\mu^{*2})$ which is also expressible as $1.341Rt/(\kappa h_n^2)$. The maximum loading of the quasi-static range is at $Rt_cW^2/(\kappa\mu^{*2}) \approx 0.038$. Both figures indicate that from time $t = 0$, slip develops stably as the loading stress increases but, above a critical point [given mathematically by equations (13) and (14)], we would have to decrease the loading stress in order for there to be quasi-static solutions with slipping length longer than h_n . This situation is similar to buckling of a structural component, and in Figure 4, the condition given by equation (13) in the previous section has been confirmed numerically. Figure 6 shows the development of the slip distribution, $\delta(x, t)$, for the same loading. The figure indicates that the slip δ is always nonnegative and the condition assumed in equation (4), $\delta > 0$, is always satisfied.

[22] Next, consider the same problem for a different loading function $q(x) = \kappa x_0^2 [1 - e^{-(x/x_0)^2}]/2$. Here $x_0 (>0)$ is

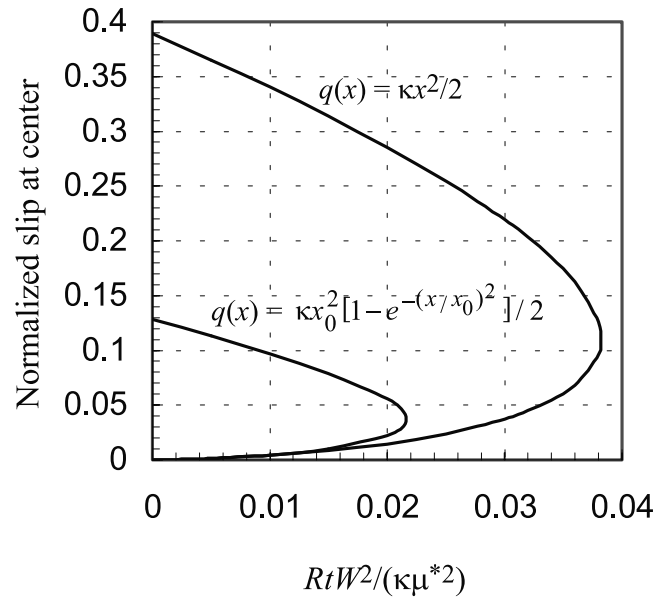


Figure 5. The development of the normalized slip at the center ($x = 0$), $W^3\delta_{cent}/(\kappa\mu^{*2})$, for two different symmetric loading distributions of $q(x)$. The normalized parameter $x_0W/\mu^* = 1/3$ for $q(x) = \kappa x_0^2 [1 - e^{-(x/x_0)^2}]/2$.

a constant that represents a reference length, and can be normalized as x_0W/μ^* . The development of the half-length aW/μ^* and the evolution of slip at the center $W^3\delta_{cent}/(\kappa\mu^{*2})$ are shown in Figures 4 and 5, respectively. The dimensionless constant x_0W/μ^* is set to $x_0W/\mu^* = 1/3$. The figures, again, indicate that the slip development has a critical point, where no further quasi-static solution exists for additional

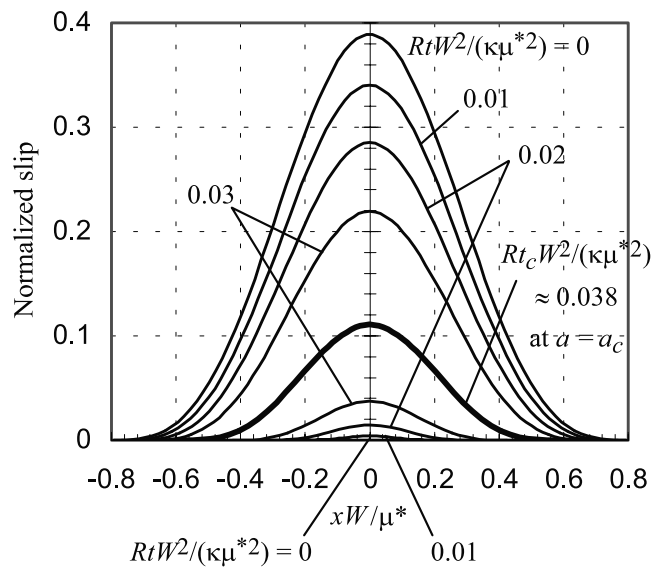


Figure 6. The development of the normalized slip distribution, $W^3\delta/(\kappa\mu^{*2})$, for loading with $q(x) = \kappa x^2/2$. The heavy line is the unstable limit to the range of existence of quasi-static solutions under monotonic increase of the loading stress.

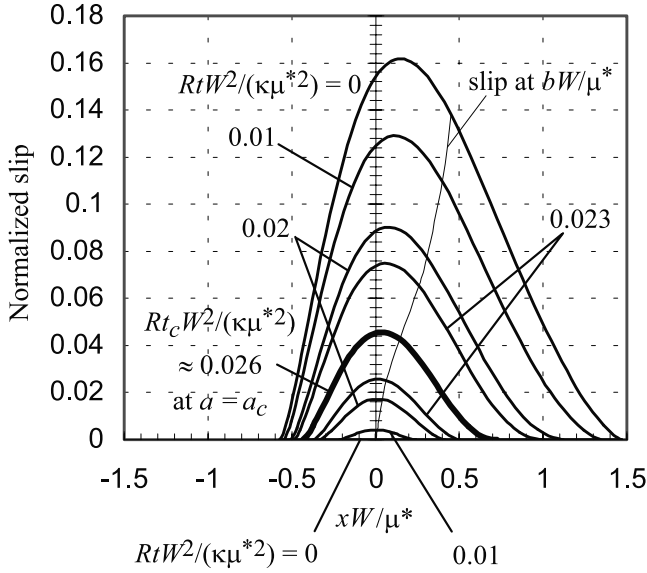


Figure 7. The development of the normalized slip distribution, $W^3\delta/(\kappa\mu^{*2})$, for the nonsymmetric loading distribution. (The normalized parameter $x_0W/\mu^* = 1/3$.) The fine line indicates the center of the slipping region, bW/μ^* , and the slip at that position. The heavy line is the unstable limit to quasi-static solutions under monotonic increase of the loading stress.

increase of the loading. However, comparison of the results obtained for the two distinct loading functions, $q(x)$, suggests that the critical stress increment Rt_c , which will render an unstable state, can differ according to the shape of the loading function, but, as forecast by the previous analysis, the critical length remains the same as given in equation (13), regardless of the shape of the function $q(x)$. Note that there is the necessity for δ_{cent} to be small enough for a linear slip-weakening range $W\delta_{cent} < \Delta\tau$ (maximum strength drop for linear range; see Figure 2), which will pose a restriction on $\kappa/\Delta\tau$. For example, for $q(x) = \kappa x^2/2$, $W^3\delta_{cent}/(\kappa\mu^{*2}) \approx 0.111$ at the critical state (see Figure 5). This implies $0.111 \approx W^3\delta_{cent}/(\kappa\mu^{*2}) < \Delta\tau W^2/(\kappa\mu^{*2})$, or $\kappa/\Delta\tau < 9.009W^2/\mu^{*2} = 12.08/h_n^2$, for $q(x) = \kappa x^2/2$. Similarly, there is a restriction $\kappa/\Delta\tau < 27.47W^2/\mu^{*2} = 36.84/h_n^2$ for $q(x) = \kappa x_0^2[1 - e^{-(x/x_0)^2}]/2$ with $x_0W/\mu^* = 1/3$.

[23] To summarize some dimensionless stress ratios, for the case $q(x) = \kappa x^2/2$, we find that $Rt_c/q(a_c) \approx 0.227$, $W\delta_{cent}/Rt_c \approx 2.921$, and $W\delta_{cent}/q(a_c) \approx 0.662$ at the critical state. Here $q(a_c)$ measures the nonuniformity of the loading stress, $W\delta_{cent}$ gives the maximum preinstability strength loss by slip-weakening (which must be checked to be in the linear range on Figure 2, i.e., $W\delta_{cent} < \Delta\tau$), and Rt_c is the increment of tectonic stressing over which preinstability slip occurs.

4.2. Nonsymmetrically Peaked Loading

[24] In the case for which the loading stress is not symmetrically peaked, the center of the slipping region, $b(t)$, moves, and the analysis becomes more complicated. Assume that $q(x)$ is nonsymmetric and described as a combination of the above two loading functions $q(x) = \kappa x^2/2$ for $x \leq 0$, and $q(x) = \kappa x_0^2[1 - e^{-(x/x_0)^2}]/2$ for $x > 0$.

Note the continuity at $x = 0$, $q(0) = q'(0) = 0$. The development of the half-length of the slipping region, aW/μ^* , is shown in Figure 4. The dimensionless constant x_0W/μ^* is set to $x_0W/\mu^* = 1/3$. In the figure, again, the critical length can be identified clearly and verified to be universal, as we have proven, regardless of the shape of the loading function $q(x)$. In Figure 7, the development of the slip distribution $\delta(x, t)$ for the same loading condition is shown. The figure indicates the nonsymmetric evolution of the slip distribution.

5. Discussion

[25] One of the major questions in the study of earthquake nucleation is whether the nucleation process and the eventual size of the ensuing earthquake are related to each other or not. Some researchers suggest that the nucleation size is related to the ultimate size of the resulting earthquake [e.g., *Ellsworth and Beroza, 1995; Ohnaka, 2000*] while others support the idea that the nucleation size is unrelated to the final size of an earthquake [*Mori and Kanamori, 1996; Kilb and Gomberg, 1999*]. Very recently, *Lapusta et al. [2000]* and Lapusta and Rice (submitted manuscript, 2002) have demonstrated, in numerical simulations of crustal earthquake sequences with depth-variable rate and state friction, that the nucleation process, in the sense of transition from initially aseismic slippage to the onset of a dynamic breakout, is virtually identical for large and small events, supporting the view that large earthquakes are small earthquakes that run away due to favorable conditions on the fault. Therefore, the nucleation length given by equation (13) may be of the same order both for laboratory experiments and for real earthquakes, small as well as large.

[26] In this section, based on equation (13), we will consider nucleation sizes associated with laboratory-derived and earthquake-inferred data sets, and also discuss the

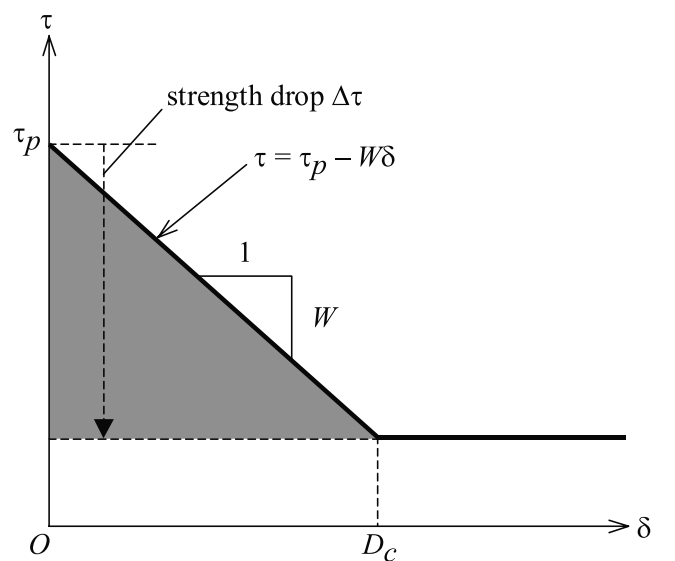


Figure 8. The linear slip-weakening constitutive law and the characteristic slip-weakening distance D_c . The slip-weakening rate W is given in terms of D_c and the strength drop $\Delta\tau$, by $W = \Delta\tau/D_c$.

validity of the widely inferred large characteristic slip-weakening distance, D_c , for the latter (see Figure 8).

5.1. Laboratory-Derived Data Sets and the Nucleation Length

[27] In our formula for the universal nucleation length (13), the slip-weakening rate W plays a crucial part. This parameter in the linear weakening friction law (3) is given by $W = \Delta\tau/D_c$ if one assumes linear weakening for slips $\delta < D_c$, and no further weakening for $\delta > D_c$.

[28] First, consider the slip-weakening process in the postfailure stage of laboratory tests of initially intact samples. *Rice* [1980] and *Wong* [1986] have evaluated the slip-weakening relation and shear fracture energy associated with the laboratory testing of shear fracture of initially intact Fichtelbirge granite specimens [*Rummel et al.*, 1978] at different confining pressures (7.5 to 300 MPa) in a stiff, servo-controlled triaxial apparatus. Their results suggest that $\mu = 30$ GPa and $\nu = 0.25$ (i.e., $\mu^* = 40$ GPa), and the slip-weakening process is approximately linear (see figures in *Rice* [1980]), except for the initial and final stages. In the relatively low range of the fault-normal compressive stress, $60 \text{ MPa} < \sigma_n < 120 \text{ MPa}$, the slip-weakening distance is approximately $D_c = 440 \text{ }\mu\text{m}$ and the strength drop $\Delta\tau = 20 \text{ MPa}$. In this case, the slip-weakening rate $W = \Delta\tau/D_c \approx 50 \text{ GPa/m}$ and the nucleation length is $h_n \approx 0.9 \text{ m}$. For $\sigma_n = 140 \text{ MPa}$, the slip-weakening distance is about $D_c = 460 \text{ }\mu\text{m}$ and the strength drop is found to be $\Delta\tau = 30 \text{ MPa}$. We have $W \approx 70 \text{ GPa/m}$ and $h_n \approx 0.7 \text{ m}$ in this instance.

[29] Under relatively high fault-normal compression $250 \text{ MPa} < \sigma_n < 600 \text{ MPa}$, D_c is some $800 \text{ }\mu\text{m}$ and the strength drop scales with σ_n , $\Delta\tau = 0.04\sigma_n + 50 \text{ MPa}$ [*Wong*, 1986]. Therefore, in this range of σ_n , $\Delta\tau \approx 60$ to 75 MPa and the slip-weakening rate is $W \approx 75$ to 90 GPa/m . Hence we have $h_n \approx 0.5$ to 0.6 m .

[30] Next, assume an established fault surface, described by a laboratory-derived rate- and state-dependent friction law with the Dieterich-Ruina-type slowness (or ageing) state evolution [*Ruina*, 1983], written as

$$\tau = \bar{\sigma}[f_o + a \ln(V/V_o) + b \ln(V_o\theta/L)], \quad d\theta/dt = 1 - V\theta/L. \quad (17)$$

Here, $\bar{\sigma}$, V , θ and L are effective normal stress, slip rate, state variable and characteristic slip distance for evolution of frictional strength, respectively, a and b are frictional parameters, and f_o is the friction coefficient at the reference rate V_o . In the case for which the state variable θ is initially large (i.e., a fault which has not recently ruptured), if slip rates are large enough to make $V\theta/L \gg 1$, then the second equation of (17) becomes $d\theta/\theta = -Vdt/L$, and, upon integration, we have $\ln(V_o\theta/L) = -\delta/L + C$. Here, δ is slip and C is a constant. By substituting this relation into the first equation of (17), we obtain

$$\tau = \bar{\sigma}[f_o + a \ln(V/V_o) + bC - b\delta/L]. \quad (18)$$

This relation (18) suggests that if the effective normal stress $\bar{\sigma}$ is constant and the slip rate V varies by less than a few powers of 10 (since $a \sim 0.01$ and $f_o \sim 0.6$), we can rewrite it approximately as in the slip-weakening law (3) with the slip-weakening rate $W = b\bar{\sigma}/L$. It has not yet been

established that a full treatment of the rate and state expressions would actually reduce to rate-independent slip-weakening in that way, at least in some special parameter range, and preliminary work by N. Lapusta (private communication, 2001) suggests that parameter a of the friction law will have to be unreasonably small to make nucleation in that context coincide closely with slip-weakening predictions. However, accepting it as an approximation, from equation (13) we have

$$h_n \approx 1.158\mu^*L/(b\bar{\sigma}). \quad (19)$$

If typical data, $\mu^* = 40 \text{ GPa}$, $\bar{\sigma} = 140 \text{ MPa}$, $b = 0.015$ and $L = 5$ to $100 \text{ }\mu\text{m}$ [see, e.g., *Marone*, 1998], are employed, then $W \approx 20$ to 420 GPa/m and the critical length is calculated to be $h_n \approx 0.1$ to 2.3 m . We notice that the results $W \approx 70 \text{ GPa/m}$ and $h_n \approx 0.7 \text{ m}$ for $\bar{\sigma} = 140 \text{ MPa}$, $b = 0.015$ and $L = 30 \text{ }\mu\text{m}$ compare well with the one obtained from the laboratory triaxial tests of initially intact Fichtelbirge granite samples ($D_c = 460 \text{ }\mu\text{m}$ and $\Delta\tau = 30 \text{ MPa}$ for $\sigma_n = 140 \text{ MPa}$), with a ratio $D_c/L \approx 15$. An initially intact Fichtelbirge granite specimen under triaxial loading conditions may thus be regarded as a fault that has not fractured recently, with the state variable θ being initially large.

[31] Adopting the rate- and state-dependent constitutive law (17), *Cocco and Bizzarri* [2002] have studied the dynamic traction behavior within the cohesive zone during their simulations of propagating earthquake ruptures and have shown that an equivalent slip-weakening distance D_c , displayed in the resulting slip-weakening curve, is related to the parameter L in the friction law (17), roughly by $D_c/L \approx 15$ also in their case. This relation indicates that if we employ laboratory-derived value of L of the order of 5 to $100 \text{ }\mu\text{m}$, then D_c at the tip of a propagating dynamic rupture is roughly of the order of $75 \text{ }\mu\text{m}$ to 1.5 mm , but there is no proof that such a scaling applies to nucleation under quasi-static loading.

5.2. Earthquake-Inferred Data Sets and the Length of Nucleation

[32] Much larger values of D_c (of order of one meter) are widely inferred in seismic inversions, using numerical calculations that simulate fault rupture, and implicitly assuming that the entire slip-weakening process is described by a linear relation like in Figure 8, but typically with the total strength drop $\Delta\tau$, or WD_c , assumed and not directly constrained from data. For example, from inversion of strong ground motion data associated with the 1995 Hyogo-ken Nanbu (Kobe), Japan, earthquake with the band-pass filter of frequency range 0.025 to 0.5 Hz , *Ide and Takeo* [1997] reported a strength drop $\Delta\tau$ of about 5 MPa and the slip-weakening distance D_c of some 1 m or more for the shallow part of the fault, and estimated an upper limit of 0.5 m for D_c on the deeper region of the fault. *Olsen et al.* [1997] gave $\Delta\tau = 12 \text{ MPa}$ and $D_c = 0.8 \text{ m}$ for the 1992 Landers, California, earthquake by the dynamic simulation of the previously obtained kinematic models of the Landers event [*Guatteri and Spudich*, 2000].

[33] However, our result, equation (13), suggests that if we assume a relatively large value of D_c , for example, $D_c = 0.1$ to 1 m , and low strength drop $\Delta\tau = 5$ to 15 MPa , which are typically adopted in numerical simulations [e.g., *Harris*

et al., 1991; *Ide and Takeo*, 1997; *Olsen et al.*, 1997], with $\mu^* = 40$ GPa, then the associated nucleation length is already $h_n \approx 0.3$ to 9 km. This size is, apparently, incompatible with existence of small-magnitude earthquakes.

[34] For these results to be accepted, it would seem that the slip-weakening process to which they refer would have to be taking place at much larger slips than control at initiation, so that the model with a single slip-weakening process is incomplete. For instance, a laboratory-like weakening at small slips may control nucleation, but further weakening (e.g., due to shear heating) may take place at slips that are much larger [Shaw and Rice, 2000], and it is possible that these are being sensed by the seismic inversions. In that connection, *Abercrombie and Rice* [2001] explained how the slip-weakening during the postnucleation phase could be extracted from data on the scaling of radiated energy, stress drop and slip with earthquake size. This is possible with the assumptions, not directly testable, that all dissipation occurs in slip on a single fault plane, and that the final static stress at each point on the fault equals the stress there in the last increment of dynamic slip. Data thus analyzed for small to moderate earthquakes (slips 1–500 mm) were shown to be roughly fit by a power law like in equation (6) with n about 0.2 to 0.4 (range from their oral report, slightly higher than 0.1 to 0.2 given in the abstract). This implies a weakening rate that is large at small slips but that diminishes continuously with increasing slip in such a way that no meaningful D_c can be defined. That same feature is seen in laboratory characterization of weakening at slips from the mm to m range in dense sand [Chambon *et al.*, 2002] and quartz rocks [Goldsby and Tullis, 2002]. Thus the linear law may not provide a good description of the postnucleation phase of seismic slip.

[35] However, even assuming the linear law, there are reasons why we must be cautious regarding such large values of D_c as are often inferred. First, from the observational point of view, *Guatteri and Spudich* [2000] have shown that estimates of slip-weakening distance D_c inferred from kinematic inversion models of earthquakes are likely to be biased large due to the effects of spatial and temporal smoothing constraints applied in such inverse problem formulations. Short periods are filtered out of the instrumental records because of contamination by scattering. *Guatteri and Spudich* [2000] have indicated that D_c is not uniquely given by seismic inversions; In order to constrain D_c , it is necessary to model ground motion spectra at frequencies higher than those at which waveform modeling is currently possible.

[36] Second, from the forward modeling point of view, D_c tends to be large due to the difficulty of simulating earthquakes. One has to simulate a fault region which is at least tens to hundreds of kilometers while resolving properly slip and rapid stress change at the tips of propagating ruptures [Lapusta *et al.*, 2000]. For example, for a laboratory-derived value of the slip-weakening distance $D_c = 800$ μm , the size of rapid slip accumulation zone at the rupture front is ~ 1 m [Rice, 1980; Wong, 1986], requiring 1000 times more grid points than to resolve $D_c = 0.8$ m. Thus one tends to use larger values of D_c in conventional numerical simulations. This indicates that if forward calculations with computationally feasible grid size are matched to seismic data, there may be a bias toward the large $D_c/\Delta\tau$ (i.e., small W) that can be resolved with such grid size because numerical artifacts

will contaminate any calculations with much smaller, but possibly realistic $D_c/\Delta\tau$ (i.e., with much larger W).

6. Conclusions

[37] The purpose of this study was to show the universal critical length that is relevant to slip-weakening fault instabilities, in circumstances for which linear slip weakening is assumed. By considering the quasi-static elastic equilibrium condition together with the linear slip-weakening friction law, we have investigated the nucleation of slip-weakening instability under a locally peaked, increasing stress field. The problem has been reduced to an eigenvalue problem and it has been indicated that the critical length relevant to instabilities of a slip-weakening fault can be expressed in terms of the smallest eigenvalue, the elastic modulus and the slip-weakening rate only. The critical loading increment, above the loading when slip initiates, has also been obtained in a simple, analytical form in terms of the eigenfunction and the loading stress. It has been shown that the fundamental nature of slip instabilities remains the same even when the type (mode I, II, or III) and the shape of the loading change. It should be noted that in this quasi-static case, the loading rate R can be a variable as long as the peak of the tectonic stress increases monotonically. Typical examples have given an insight into the actual length of such instability, and it has been pointed out that the widely inferred large characteristic slip-weakening distance might be biased high due to the technical constraints employed in seismic inversions and numerical simulations. Although the problem investigated in this contribution is quite simplified, it still retains the essential characteristics that are believed to play an important part during the earthquake nucleation process.

Appendix A: Finiteness Condition and Slip Distribution Near the Ends

[38] The inverse form of equation (1) [see. e.g., *Muskheleshvili*, 1946, 1953; *Bilby and Eshelby*, 1968; *Rice*, 1968, 1980] indicates, very near the ends of the slipping region [$x = a_{\pm}(t)$],

$$\frac{\partial\delta(x,t)}{\partial x} = -\frac{2}{\pi\mu^*\sqrt{a_+(t)-a_-(t)}\sqrt{\pm[a_{\pm}(t)-x]}} \cdot \int_{a_-(t)}^{a_+(t)} \frac{\tau(\xi,t) - \tau_o(\xi,t)}{\sqrt{-a_-(t) + \xi}\sqrt{a_+(t) - \xi}} [a_{\mp}(t) - \xi] d\xi, \quad (\text{A1})$$

holds. Since the stress (and, related to it, $\partial\delta/\partial x$) must be finite at the ends, all acceptable solutions must satisfy

$$\int_{a_-(t)}^{a_+(t)} \frac{\tau(\xi,t) - \tau_o(\xi,t)}{\sqrt{-a_-(t) + \xi}\sqrt{a_+(t) - \xi}} d\xi = 0 \quad \text{and} \\ \int_{a_-(t)}^{a_+(t)} \frac{\tau(\xi,t) - \tau_o(\xi,t)}{\sqrt{-a_-(t) + \xi}\sqrt{a_+(t) - \xi}} \xi d\xi = 0, \quad (\text{A2})$$

which implies that $\partial\delta(x,t)/\partial x \sim \sqrt{\pm[a_{\pm}(t)-x]}$ or that $\delta(x,t) \sim (\pm[a_{\pm}(t)-x])^{3/2}$ for x near $a_{\pm}(t)$. Note, if the

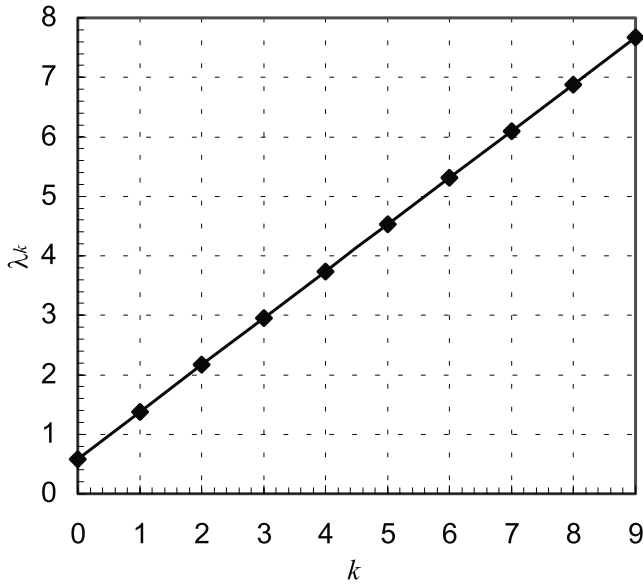


Figure B1. Eigenvalues λ_k associated with equation (B1). The λ_k increase in a manner that is almost, but not precisely, linear in k . The increment between successive value is, numerically, very close to $\pi/4$.

loading stress $\tau_o(x, t)$ is symmetric with respect to $x = 0$, then $\tau(x, t)$ is also symmetric with respect to $x = 0$ and the second equation of (A2) is automatically satisfied.

Appendix B: The Eigen Equation and the Eigenfunctions

B1. Orthogonality of the Eigenfunctions

[39] Consider the eigen equation related to equation (12)

$$\frac{1}{2\pi} \int_{-1}^{+1} \frac{v'_k(s)}{X-s} ds = \lambda_k v_k(X) \quad \text{for } -1 < X < +1, \quad (\text{B1})$$

where λ_k and $v_k(X)$ are the k -th eigenvalue and eigenfunction related to the equation, respectively ($k = 0, 1, 2, \dots$). Letting A represent the operator in equation (B1) and performing the change of order of integration, we notice that the operator is self-adjoint, $(Au, v) = (u, Av)$, with u and v vanishing at the ends, relative to the inner product $(u, v) = \int_{-1}^{+1} u(X)v(X)dX$. That leads to

$$(\lambda_k - \lambda_l) \int_{-1}^{+1} v_k(X)v_l(X)dX = 0, \quad (\text{B2})$$

implying that all eigenvalues are real and if $\lambda_k \neq \lambda_l$, $(v_k, v_l) = 0$. Operator A is also positive-definite, which follows because (Au, u) is proportional to the elastic strain energy induced by enforcing slip u along a cut in an otherwise unstressed solid, and therefore, we can arrange those eigenvalues in order so that $0 < \lambda_0 < \lambda_1 < \lambda_2 < \dots$ holds.

[40] Figures B1 and B2 show the eigenvalues λ_k and eigenfunctions $v_k(X)$ that are obtained numerically by employing the simplest discretization method with piecewise constant slip in cells of uniform size: equation (B1) is discretized as $K_{ij}v_k(j\Delta x) = \lambda_k v_k(i\Delta x)$ ($-1/\Delta x < i, j < +1/\Delta x$; summation convention is used) and solved. Here Δx is grid

spacing and $K_{ij} = -1/\{2\pi\Delta x [(i-j)^2 - 0.25]\}$. We used 163 grid points to obtain Figures B1 and B2. As indicated in section D3, the numerical difference between this discretization method and the Chebyshev polynomial approach is practically negligible. Figure B1 indicates that eigenvalues increase almost linearly with increasing number k while Figure B2 shows that the eigenfunctions are either symmetric (for even k) or anti-symmetric (for odd k) [If $v_k(X)$ is an eigenfunction, then so is $v_k(-X)$. Therefore, if only one eigenfunction exists per eigenvalue, $v_k(-X) = \pm v_k(X)$]. Each eigenfunction takes the value zero at the ends of the slipping region, i.e., $v_k(X = \pm 1) = 0$, and is normalized so

$$\int_{-1}^{+1} v_k^2(X)dX = 1. \quad (\text{B3})$$

B2. Some Characteristics of the Eigenfunctions

[41] Similarly to the derivation of (A1), the inverse form of equation (B1) is given by

$$v'_k(X) = -\frac{2}{\pi} \frac{\lambda_k}{\sqrt{1-X^2}} \int_{-1}^{+1} \frac{v_k(s)\sqrt{1-s^2}}{X-s} ds. \quad (\text{B4})$$

This shows that the $v'_k(X)$ are singular at the ends, in proportion to $\pm 1/\sqrt{1-|X|}$, suggesting that at those ends, analogous to the corresponding results in elastic crack theory, we can define “stress intensity factors” associated with the k -th eigenfunction $v_k(X)$ (see also Appendix C2).

[42] Using equation (B4) and performing some mathematical manipulations of integrals, we can show that the following relations associated with the eigenfunctions hold

$$\int_{-1}^{+1} v_k(X)v'_l(X)dX = \begin{cases} 0, & \text{if both modes are odd or both even, including } k = l \\ -\frac{\sqrt{\lambda_k\lambda_l}}{\lambda_k - \lambda_l}, & \text{if one mode is odd and the other is even} \end{cases} \quad (\text{B5})$$

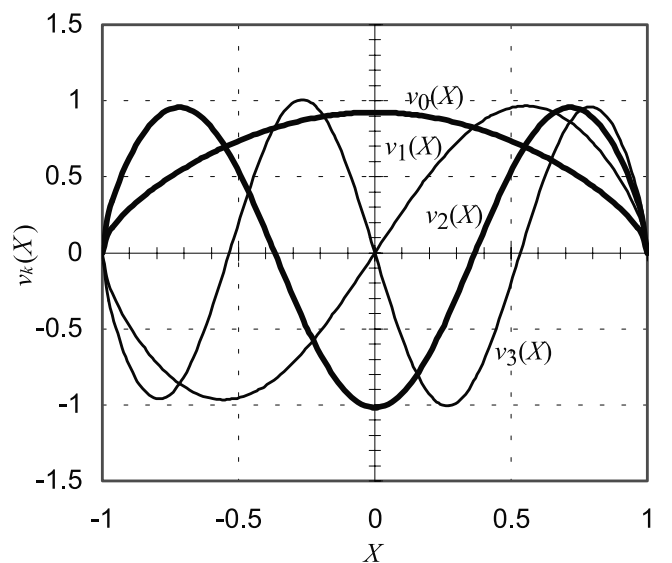


Figure B2. Eigenfunctions $v_k(X)$ related to equation (B1).

and

$$\int_{-1}^{+1} Xv_k(X)v_l'(X)dX = \begin{cases} -\frac{1}{2}, & \text{if both are the same mode, i.e } k = l \\ 0, & \text{if one mode is odd and the other is even} \\ -\frac{\sqrt{\lambda_k\lambda_l}}{\lambda_k - \lambda_l}, & \text{if the modes are distinct } (k \neq l) \\ & \text{and either both odd or both even.} \end{cases} \quad (\text{B6})$$

The above two equations imply the eigen-expansions

$$v_l'(X) = -\sum_{k=0}^{\infty} \frac{\sqrt{\lambda_k\lambda_l}}{\lambda_k - \lambda_l} v_k(X), \quad (\text{B7})$$

(l even and k odd, or l odd and k even)

and

$$Xv_l'(X) = -\frac{1}{2}v_l(X) - \sum_{\substack{k=0 \\ k \neq l}}^{\infty} \frac{\sqrt{\lambda_k\lambda_l}}{\lambda_k - \lambda_l} v_k(X), \quad (\text{B8})$$

(l, k both even or both odd)

respectively.

Appendix C: Critical Stress Increment Rt_c

C1. The Problem in Terms of the Eigenfunctions

[43] By decomposing the slip distribution $\delta(x, t)$ in terms of the eigenfunctions $v_k(X)$ as

$$\delta(x, t) = \sum_{k=0}^{\infty} A_k v_k(X), \quad (\text{C1})$$

we can rewrite equation (4) as

$$-W \sum_{k=0}^{\infty} A_k v_k(X) = Rt - q(a(t)X + b(t)) - \frac{\mu^*}{a(t)} \sum_{k=0}^{\infty} \lambda_k A_k v_k(X). \quad (\text{C2})$$

Multiplying $v_k(X)$, integrating from -1 to $+1$ and using equation (B3), we obtain

$$A_k = \frac{a(t)[\beta_k Rt - Q_k(a(t), b(t))]}{W[a_k - a(t)]}. \quad (\text{C3})$$

Here, $Q_k(a(t), b(t))$, a_k and β_k are defined by $Q_k(a, b) \equiv \int_{-1}^{+1} q(aX + b)v_k(X)dX$, $a_k \equiv \lambda_k \mu^*/W$ and $\beta_k \equiv \int_{-1}^{+1} v_k(X)dX$, respectively. Note that due to antisymmetric nature of the odd mode eigenfunctions, $\beta_k = 0$ for odd k . In the following, the finiteness condition will be considered in terms of A_k and then equation (C3) will be used in order to obtain the critical condition associated with the quasi-static slip-weakening problem.

C2. Finiteness Condition

[44] In order to have no singularity of stress at the ends of the slipping region [$x = a_{\pm}(t)$, or $X = \pm 1$], from a fracture

mechanics point of view, it is necessary that the following condition be satisfied

$$\sum_{k=0}^{\infty} A_k (K_R)_k = 0 \quad \text{and} \quad \sum_{k=0}^{\infty} A_k (K_L)_k = 0. \quad (\text{C4})$$

Here, $(K_R)_k$ and $(K_L)_k$ are the ‘‘stress intensity factors,’’ associated with k -th eigenfunction $v_k(X)$, at the right ($x = a_+$, or $X = +1$) and left ($x = a_-$, or $X = -1$) end of the slipping region, respectively. These are defined, in analogy to the corresponding results in elastic crack theory, by $(K_{R,L})_k = \lim_{X \rightarrow \pm 1} [\mp \mu^* \sqrt{\pi a/2} \sqrt{1 - |X|} v_k'(X)]$. Utilizing this near tip slip-stress intensity factor relation and equations (B4), (B5), and (B6), and after some mathematical calculations, we notice $(K_R)_k^2 = (K_L)_k^2 = \mu^{*2} a(t) \lambda_k/2$ holds. This relation indicates the (anti) symmetric nature of the eigenfunctions. Adopting a convention K_R is always positive and K_L may be positive (even mode) or negative (odd mode), the finiteness condition (C4) reads

$$\sum_{k=0}^{\infty} A_k \sqrt{\lambda_k} = 0 \quad \text{and} \quad \sum_{k=0}^{\infty} A_k (-1)^k \sqrt{\lambda_k} = 0. \quad (\text{C5})$$

Using equation (C3) and noting that λ_k is proportional to a_k ($\equiv \lambda_k \mu^*/W$) and $\beta_k = 0$ for odd k , we can rewrite this condition (C5) as

$$\sum_{k=0,2,4,\dots}^{\infty} \frac{\sqrt{a_k} [\beta_k Rt - Q_k(a(t), b(t))]}{a_k - a(t)} = 0 \quad \text{and} \quad \sum_{k=1,3,5,\dots}^{\infty} \frac{\sqrt{a_k} Q_k(a(t), b(t))}{a_k - a(t)} = 0. \quad (\text{C6})$$

C3. Nucleation Length and Critical Stress Increment

[45] Consider the derivatives of $Q_l(a, b) \equiv \int_{-1}^{+1} q(aX + b)v_l(X)dX$. From equation (B8), the following relation holds

$$a \frac{\partial Q_l(a, b)}{\partial a} = -Q_l(a, b) - \int_{-1}^{+1} q(aX + b)Xv_l'(X)dX = -\frac{1}{2}Q_l(a, b) + \sum_{\substack{k=0 \\ k \neq l}}^{\infty} \frac{\sqrt{a_k a_l}}{a_k - a_l} Q_k(a, b). \quad (\text{C7})$$

(l, k both even or both odd)

Applying the above equation (C7) to the case $q(x) = 1$ and noting that $\beta_l = \beta_k = 0$ if l and k are odd, we have $Q_l(a, b) = \beta_l$, $Q_k(a, b) = \beta_k$, $\partial Q_l(a, b)/\partial a = 0$, and

$$\sum_{\substack{k=0 \\ k \neq l}}^{\infty} \frac{\sqrt{a_k a_l} \beta_k}{a_k - a_l} = \frac{1}{2}. \quad (\text{C8})$$

(l, k both even)

Similarly, from equation (B7),

$$a \frac{\partial Q_l(a, b)}{\partial b} = - \int_{-1}^{+1} q(aX + b)v_l'(X)dX = \sum_{k=0}^{\infty} \frac{\sqrt{a_k a_l}}{a_k - a_l} Q_k(a, b). \quad (\text{C9})$$

(l even and k odd, or l odd and k even)

[46] Let us now consider the first finiteness condition of (C6), which gives Rt as a function of a and b . Near $a = a_l$

and $\beta_l Rt = Q_l(a_l, b)$ where l is even (both the numerator and denominator in the first of (C6) must vanish when $a = a_l$),

$$\begin{aligned} & \beta_l Rt(a_l, b) - Q_l(a_l, b) \\ &= \left[\beta_l \left(\frac{\partial Rt(a, b)}{\partial a} \right)_{a=a_l} - \left(\frac{\partial Q_l(a, b)}{\partial a} \right)_{a=a_l} \right] (a - a_l). \end{aligned} \quad (C10)$$

That first finiteness condition can then be expressed as

$$\begin{aligned} a_l \beta_l \left(\frac{\partial Rt(a, b)}{\partial a} \right)_{a=a_l} &= a_l \left(\frac{\partial Q_l(a, b)}{\partial a} \right)_{a=a_l} + Q_l(a_l, b) \sum_{\substack{k=0 \\ k \neq l}}^{\infty} \frac{\sqrt{a_k a_l} \beta_k}{a_k - a_l} \beta_l \\ &- \sum_{\substack{k=0 \\ k \neq l}}^{\infty} \frac{\sqrt{a_k a_l}}{a_k - a_l} Q_k(a_l, b). \quad (l, k \text{ both even}) \end{aligned} \quad (C11)$$

From equations (C7) and (C8), we obtain

$$\begin{aligned} a_l \beta_l \left(\frac{\partial Rt(a, b)}{\partial a} \right)_{a=a_l} &= a_l \left(\frac{\partial Q_l(a, b)}{\partial a} \right)_{a=a_l} \\ &+ \frac{1}{2} Q_l(a_l, b) - \left[a_l \left(\frac{\partial Q_l(a, b)}{\partial a} \right)_{a=a_l} + \frac{1}{2} Q_l(a_l, b) \right] = 0. \quad (l \text{ even}) \end{aligned} \quad (C12)$$

The conditions $\partial[Rt(a, b)]/\partial a = 0$ at $a = a_l$ and $\beta_l Rt(a_l, b) = Q_l(a_l, b)$ follow from the first of (C6) for even l no matter what value is read in for the center location b of the slipping zone. However, the second of (C6) expresses b in terms of a , thus giving the b_l corresponding to any a_l when l is even, and that relation is

$$\sum_{k=1}^{\infty} \frac{\sqrt{a_k} Q_k(a_l, b_l)}{a_k - a_l} = 0. \quad (l \text{ even and } k \text{ odd}) \quad (C13)$$

Using equation (C9), we can rewrite this condition as

$$\left(\frac{\partial Q_l(a, b)}{\partial b} \right)_{a=a_l, b=b_l} = 0. \quad (l \text{ even}) \quad (C14)$$

Therefore, the critical condition is given for even l by $a = a_l \equiv \lambda_l \mu^*/W$, $b = b_l$ [where $(\partial Q_l(a, b)/\partial b)_{a=a_l, b=b_l} = 0$] and $Rt = Q_l(a_l, b_l)/\beta_l$. Further, by a derivation like in (C11) and (C12) for the total derivative $d(Rt)/da = \partial(Rt)/\partial a + [\partial(Rt)/\partial b] db/da$, with db/da constrained by the second of (C6), one readily derives on the basis of (C14) that $d(Rt)/da = 0$ at $a = a_l$ and $b = b_l$.

[47] In reality, as the slipping region develops, the critical length associated with the smallest eigenvalue is first reached. Since $d(Rt)/da$ first decreases to 0 then, it is the instability length. Therefore, the condition $a_c = a_0 \equiv \lambda_0 \mu^*/W$, $b_c = b_0$ [$\partial Q_0(a, b)/\partial b = 0$ at $a = a_c$, $b = b_c$] and $Rt_c = Q_0(a_c, b_c)/\beta_0$ (equation (14)) is of practical importance. Note that the expressions for a_c , b_c and the critical load increment Rt_c apply also for general time-variable loading so long as quasi-static conditions prevail up to just before instability. The principal results shown in this appendix can also be obtained, if not necessarily at greater economy, by using the path-independent M

integral approach in fracture mechanics [Knowles and Sternberg, 1972; Budiansky and Rice, 1973].

Appendix D: Chebyshev Polynomial Representation of the Problem

[48] In Appendix D, the equilibrium condition (4) and the finiteness condition (A2) are considered in terms of a Chebyshev polynomial representation.

D1. Finiteness Condition

[49] We define $a(t) \equiv [a_+(t) - a_-(t)]/2$, $b(t) \equiv [a_+(t) + a_-(t)]/2$ and $x_o \equiv x - b(t)$. Introducing $x_o = a(t) \cos \omega$ ($0 < \omega < \pi$) and the slip distribution of the form

$$\delta(x_o, t) = \sum_{n=1}^{\infty} u_n(t) \sin(n\omega), \quad (0 < \omega < \pi) \quad (D1)$$

and using the integral formula $\int_0^\pi \frac{\cos(n\theta)}{\cos\theta - \cos\omega} d\theta = \pi \frac{\sin(n\omega)}{\sin\omega}$, we can rewrite equation (1) as

$$\begin{aligned} \tau(x_o, t) - \tau_o(x_o, t) &= -\frac{\mu^*}{2\pi} \int_{-a(t)}^{+a(t)} \frac{\partial \delta(\eta, t)/\partial \eta}{x_o - \eta} d\eta \\ &= -\frac{\mu^*}{2a(t)} \sum_{n=1}^{\infty} n u_n(t) \frac{\sin(n\omega)}{\sin\omega}. \quad (0 < \omega < \pi) \end{aligned} \quad (D2)$$

From this relation and the finiteness condition (A2), it is necessary that

$$\begin{aligned} & \int_{-a(t)}^{+a(t)} \frac{\tau(\eta, t) - \tau_o(\eta, t)}{\sqrt{a^2(t) - \eta^2}} d\eta = \\ & -\frac{\mu^*}{2a(t)} \sum_{n=1}^{\infty} n u_n(t) \int_0^\pi \frac{\sin(n\theta)}{\sin\theta} d\theta = 0, \text{ and} \end{aligned} \quad (D3)$$

$$\begin{aligned} & \int_{-a(t)}^{+a(t)} \frac{\tau(\eta, t) - \tau_o(\eta, t)}{\sqrt{a^2(t) - \eta^2}} \eta d\eta = \\ & -\frac{\mu^*}{2} \sum_{n=1}^{\infty} n u_n(t) \int_0^\pi \frac{\sin(n\theta)}{\sin\theta} \cos\theta d\theta = 0. \end{aligned}$$

Noting that $\int_0^\pi \frac{\sin(n\theta)}{\sin\theta} d\theta = \pi$ for odd n and 0 for even n , and $\int_0^\pi \frac{\sin(n\theta)}{\sin\theta} \cos\theta d\theta = \pi$ for even n ($n > 1$) and 0 otherwise, we can express the condition (D3) as

$$\sum_{n=1,3,5,\dots}^{\infty} n u_n(t) = 0 \text{ and } \sum_{n=2,4,6,\dots}^{\infty} n u_n(t) = 0. \quad (D4)$$

If the coefficients $u_n(t)$ satisfy the above finiteness condition (D4), we have no stress singularity at the ends of the slipping region. Related expressions are given by Erdogan and Gupta [1972] in presenting a method for numerical solution of singular integral equations, and by Dascalu et al. [2000] in discussing the initial dynamic motion of a uniformly, and critically, stressed fault segment.

D2. Elastic Equilibrium

[50] From the equilibrium condition (4) and equation (D2), we have

$$\begin{aligned}
& Rt - q(a(t) \cos \omega + b(t)) \\
&= \sum_{n=1}^{\infty} \left(\frac{n\mu^*}{2a(t) \sin \omega} - W \right) u_n(t) \sin(n\omega). \quad (0 < \omega < \pi) \quad (D5)
\end{aligned}$$

Multiplying $\sin(m\omega)$ and then integrating from 0 to π , we obtain

$$\begin{aligned}
& \int_0^{\pi} [Rt - q(a(t) \cos \omega + b(t))] \sin(m\omega) d\omega \\
&= \sum_{n=1}^{\infty} \left[\frac{n\mu^*}{2a(t)} \int_0^{\pi} \frac{\sin(m\omega) \sin(n\omega)}{\sin \omega} d\omega \right. \\
&\quad \left. - W \int_0^{\pi} \sin(m\omega) \sin(n\omega) d\omega \right] u_n(t). \quad (D6)
\end{aligned}$$

Noting that $\int_0^{\pi} \sin(m\omega) \sin(n\omega) d\omega = \pi/2$ if $m = n$ and 0 if $m \neq n$, we can rewrite this equation (D6) as

$$b_m = \sum_{n=1}^{\infty} A_{mn} u_n(t), \quad (D7)$$

where the matrix \mathbf{A}

$$A_{mn} = \frac{n\mu^*}{2a(t)} I(m, n) - W \frac{\pi}{2} \delta_{m,n}, \quad (D8)$$

$I(m, n) \equiv \int_0^{\pi} \frac{\sin(m\omega) \sin(n\omega)}{\sin \omega} d\omega$, $\delta_{m,n}$ is 1 if $m = n$ and 0 if $m \neq n$, and the vector \mathbf{b}

$$b_m = \frac{Rt}{m} [1 - (-1)^m] - \int_0^{\pi} q(a(t) \cos \omega + b(t)) \sin(m\omega) d\omega. \quad (D9)$$

For numerical evaluation of equation (D7) we retain the first N terms in the series so that we have $(N + 2)$ simultaneous equations, (D4) and (D7), for $(N + 2)$ unknown variables, $u_n(t)$, $a(t)$ and $b(t)$. Then we can numerically solve the simultaneous equations under different values of stress increment, Rt . Note that for a symmetric form of $q(x)$, $b(t) = 0$, $u_n(t) = 0$ for even n , and $I(m, n) = 0$ if either m or n (not both of them) is even. In producing Figures 4–7, the first $N = 5$ terms in the series of equation (D7) are used. Any increase of N does not change the overall result.

D3. Expression for the First Eigenfunction

[51] The results in Figures B1 and B2 were obtained by numerically discretizing equation (B1). Alternatively, the same Chebyshev polynomial representation can be used to obtain the eigenvalues (for which derivatives are not subject to the finiteness condition at the ends). In view of equation (14), $v_0(X)$ is of primary interest. It is found to be given, to sufficient accuracy, by

$$\begin{aligned}
v_0(X) \approx & v_{01} \sin \omega + v_{02} \sin 2\omega + v_{03} \sin 3\omega = 0.848 \sin \omega \\
& - 0.077 \sin 3\omega = (0.925 - 0.308X^2) \sqrt{1 - X^2}, \quad (D10)
\end{aligned}$$

where $X = \cos \omega$, $-1 < X < +1$ and $0 < \omega < \pi$. From that result, we obtain $\beta_0 = (\pi/2) v_{01} \approx 1.332$. Comparison of

the numerical values obtained by two different methods, one by discretization described in Appendix B1 and the other by equation (D10), shows that the difference between those two methods is practically negligible: 0.16% for $v_0(0)$ and 0.06% for β_0 . For the symmetric loading $q(x) = \kappa x^2/2$, from equation (14), we have $Q_0(a, 0) = (\pi/16) \kappa a^2 (v_{01} + v_{03}) \approx 0.151 \kappa a^2$ and the critical stress increment $Rt_c = Q_0(a_c, 0)/\beta_0 = \kappa a_c^2 (v_{01} + v_{03})/(8v_{01}) \approx 0.038 \kappa \mu^{*2}/W^2$. This result, which can also be obtained using equation (15), is consistent with the ones shown in section 4.1 and Figures 4–6.

[52] **Acknowledgments.** Support by the Southern California Earthquake Center (SCEC), by NSF through grant EAR-0125709, and, for K. U., by the Japan Society for the Promotion of Science (JSPS) Postdoctoral Fellowships for Research Abroad 2000–2002 is gratefully acknowledged. We are grateful for discussions in the early stages of this work with Jean-Paul Ampuero of IPG/Paris, who noted that our quasi-static eigen problem was identical to that of Campillo, Ionescu and coworkers, and for his comments on a semifinal version of the manuscript. Also, we are grateful for discussions with Nadia Lapusta of Harvard on nucleation in the rate and state context.

References

- Abercrombie, R. E., and J. R. Rice, Small earthquake scaling revisited: Can it constrain slip weakening?, *Eos Trans. AGU*, 82(47), Fall Meet. Suppl., Abstract S21E-04, 2001.
- Bazant, Z. P., and Y.-N. Li, Stability of cohesive crack model, 1, Energy principles, *J. Appl. Mech.*, 62, 959–964, 1995a.
- Bazant, Z. P., and Y.-N. Li, Stability of cohesive crack model, 2, Eigenvalue analysis of size effect on strength and ductility of structures, *J. Appl. Mech.*, 62, 965–969, 1995b.
- Bilby, B. A., and J. D. Eshelby, Dislocations and theory of fracture, in *Fracture, An Advanced Treatise*, vol. 1, edited by H. Liebowitz, pp. 99–182, Academic, San Diego, Calif., 1968.
- Budiansky, B., and J. R. Rice, Conservation laws and energy-release rates, *J. Appl. Mech.*, 40, 201–203, 1973.
- Campillo, M., and I. R. Ionescu, Initiation of antiplane shear instability under slip dependent friction, *J. Geophys. Res.*, 102, 20,363–20,371, 1997.
- Chambon, G., J. Schmittbuhl, and A. Corfdir, Laboratory gouge friction: seismic-like slip weakening and secondary rate- and state-effects, *Geophys. Res. Lett.*, 29, doi:10.1029/2001GL014467, in press, 2002.
- Cocco, M., and A. Bizzarri, On the slip-weakening behavior of rate- and state-dependent constitutive laws, *Geophys. Res. Lett.*, 29, doi:10.1029/2001GL013999, in press, 2002.
- Dascalu, C., I. R. Ionescu, and M. Campillo, Fault finiteness and initiation of dynamic shear instability, *Earth Planet. Sci. Lett.*, 177, 163–176, 2000.
- Dieterich, J. H., Earthquake nucleation on faults with rate- and state-dependent strength, *Tectonophysics*, 211, 115–134, 1992.
- Ellsworth, W. L., and G. C. Beroza, Seismic evidence for an earthquake nucleation phase, *Science*, 268, 851–855, 1995.
- Erdogan, F., and G. D. Gupta, On the numerical solution of singular integral equations, *Q. Appl. Math.*, 29, 525–534, 1972.
- Favreau, P., M. Campillo, and I. R. Ionescu, Initiation of in-plane shear instability under slip-dependent friction, *Bull. Seismol. Soc. Am.*, 89, 1280–1295, 1999.
- Goldsby, D. L., and T. E. Tullis, Low frictional strength of quartz rocks at subseismic slip rates, *Geophys. Res. Lett.*, 29, doi:10.1029/2002GL015240, in press, 2002.
- Guatteri, M., and P. Spudich, What can strong motion data tell us about slip-weakening fault friction laws?, *Bull. Seismol. Soc. Am.*, 90, 98–116, 2000.
- Harris, R. A., R. J. Archuleta, and S. M. Day, Fault steps and the dynamic rupture process: 2-D numerical simulations of a spontaneously propagating shear fracture, *Geophys. Res. Lett.*, 18, 893–896, 1991.
- Ide, S., and M. Takeo, Determination of constitutive relations of fault slip based on seismic wave analysis, *J. Geophys. Res.*, 102, 27,379–27,391, 1997.
- Ionescu, I. R., and M. Campillo, Influence of the shape of friction law and fault finiteness on the duration of initiation, *J. Geophys. Res.*, 104, 3013–3024, 1999.
- Kilb, D., and J. Gombert, The initial subevent of the 1994 Northridge, California, earthquake: Is earthquake size predictable?, *J. Seismol.*, 3, 409–420, 1999.

- Knowles, J. K., and E. Sternberg, On a class of conservation laws in linearized and finite elastostatics, *Arch. Ration. Mech. Anal.*, *44*, 187–211, 1972.
- Lapusta, N., J. R. Rice, Y Ben-Zion, and G. Zheng, Elastodynamic analysis for slow tectonic loading with spontaneous rupture episodes on faults with rate- and state-dependent friction, *J. Geophys. Res.*, *105*, 23,765–23,789, 2000.
- Li, Y. N., and R. Y. Liang, The theory of the boundary eigenvalue problem in the cohesive crack model and its application, *J. Mech. Phys. Solids*, *41*, 331–350, 1993.
- Marone, C., Laboratory-derived friction laws and their application to seismic faulting, *Annu. Rev. Earth Planet. Sci.*, *26*, 643–696, 1998.
- Mori, J., and H. Kanamori, Initial rupture of earthquakes in the 1995 Ridgecrest, California sequence, *Geophys. Res. Lett.*, *23*, 2437–2440, 1996.
- Muskhelishvili, N. I., *Singular Integral Equations*, translated by J. R. M. Radok, 447 pp., P. Noordhoff, Groningen, Netherlands, 1946.
- Muskhelishvili, N. I., *Some Basic Problems of the Mathematical Theory of Elasticity*, translated by J. R. M. Radok, 704 pp., P. Noordhoff, Groningen, Netherlands, 1953.
- Ohnaka, M., A physical scaling relation between the size of an earthquake and its nucleation zone size, *Pure Appl. Geophys.*, *157*, 2259–2282, 2000.
- Okubo, P. G., Dynamic rupture modeling with laboratory-derived constitutive relations, *J. Geophys. Res.*, *94*, 12,321–12,335, 1989.
- Olsen, K. B., R. Madariaga, and R. J. Archuleta, Three-dimensional dynamic simulation of the 1992 Landers earthquake, *Science*, *278*, 834–838, 1997.
- Rice, J. R., Mathematical analysis in the mechanics of fracture, in *Fracture, An Advanced Treatise*, vol. 2, edited by H. Liebowitz, pp. 191–311, Academic, San Diego, Calif., 1968.
- Rice, J. R., The mechanics of earthquake rupture, in *Physics of the Earth's Interior*, edited by A. M. Dziewonski and E. Boschi, pp. 555–649, Ital. Phys. Soc./North-Holland, New York, 1980.
- Rice, J. R., and Y. Ben-Zion, Slip complexity in earthquake fault models, *Proc. Natl. Acad. Sci. U.S.A.*, *93*, 3811–3818, 1996.
- Rice, J. R., and K. Uenishi, Slip development and instability on a heterogeneously loaded fault with power-law slip-weakening, *Eos Trans. AGU*, *83*(47), Fall Meet. Suppl., abstract S61E-06, 2002.
- Ruina, A., Slip instability and state variable friction laws, *J. Geophys. Res.*, *88*, 10,359–10,370, 1983.
- Rummel, F., H. J. Alheid, and C. Frohn, Dilatancy and fracture-induced velocity changes in rock and their relation to frictional sliding, *Pure Appl. Geophys.*, *116*, 743–764, 1978.
- Shaw, B. E., and J. R. Rice, Existence of continuum complexity in the elastodynamics of repeated fault ruptures, *J. Geophys. Res.*, *105*, 23,791–23,810, 2000.
- Shibazaki, B., and M. Matsu`ura, Transition process from nucleation to high-speed rupture propagation: Scaling from stick-slip experiments to natural earthquakes, *Geophys. J. Int.*, *132*, 14–30, 1998.
- Tse, S. T., and J. R. Rice, Crustal earthquake instability in relation to the depth variation of frictional slip properties, *J. Geophys. Res.*, *91*, 9452–9472, 1986.
- Wong, T.-F., On the normal stress dependence of the shear fracture energy, in *Earthquake Source Mechanics*, edited by S. Das, J. Boatwright, and C. H. Scholz, pp. 1–11, AGU, Washington, D. C., 1986.

J. R. Rice and K. Uenishi, Department of Earth and Planetary Sciences and Division of Engineering and Applied Sciences, Harvard University, 29 Oxford Street, Cambridge, MA 02138, USA. (rice@esag.harvard.edu; uenishi@esag.harvard.edu)